



Non-strange dibaryons studied in coherent double neutral-pion photoproduction on the deuteron

Takatsugu ISHIKAWA

**Research Center for Electron Photon Science (ELPH),
Tohoku University, Japan**



**12th International Workshop on
the Physics of Excited Nucleons (NSTAR2019)**

10~14 June 2019, Bonn, Germany



Contents

$$\gamma d \rightarrow \pi^0 \pi^0 d$$

1. dibaryons
2. isocalar dibaryon $\mathcal{D}_{03}(2380)$
3. isovector $\mathcal{D}_{12}(2150)$ T. Ishikawa et al.,
PLB772, 398 (2017);
PLB789, 413 (2019).
4. experimental setup
5. total cross section
 - ~ isoscalar dibaryons $\pi^0 \pi^0 d$
6. differential cross section
 - ~ isovector dibaryons $\pi^0 d$
7. properties of the dibaryon
observed in πd system
8. summary

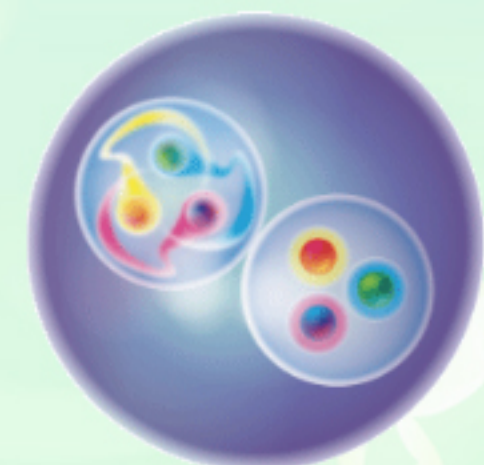
Dibaryons

a dibaryon

an object with baryon number $B=2$

deuteron is the first dibaryon
proton and neutron bound system
with spin $J=1$ and isospin $I=0$

the quark picture of a dibaryon
is of interest in the non-perturbative
domain of QCD

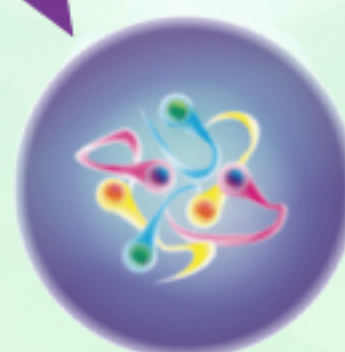
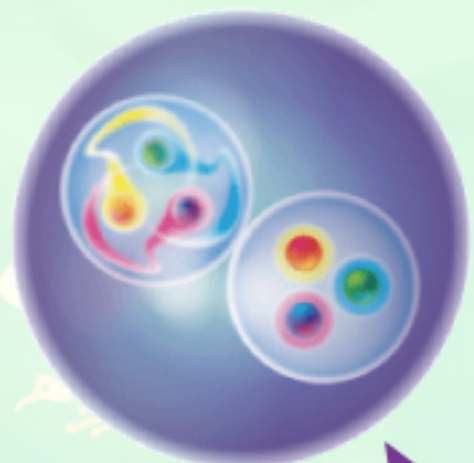




Dibaryons

a dibaryon ($B=2$ system):

a phase change of its basic configuration



a **molecule-like state**
consisting of two baryons
such as the deuteron

a **hexaquark hadron state**

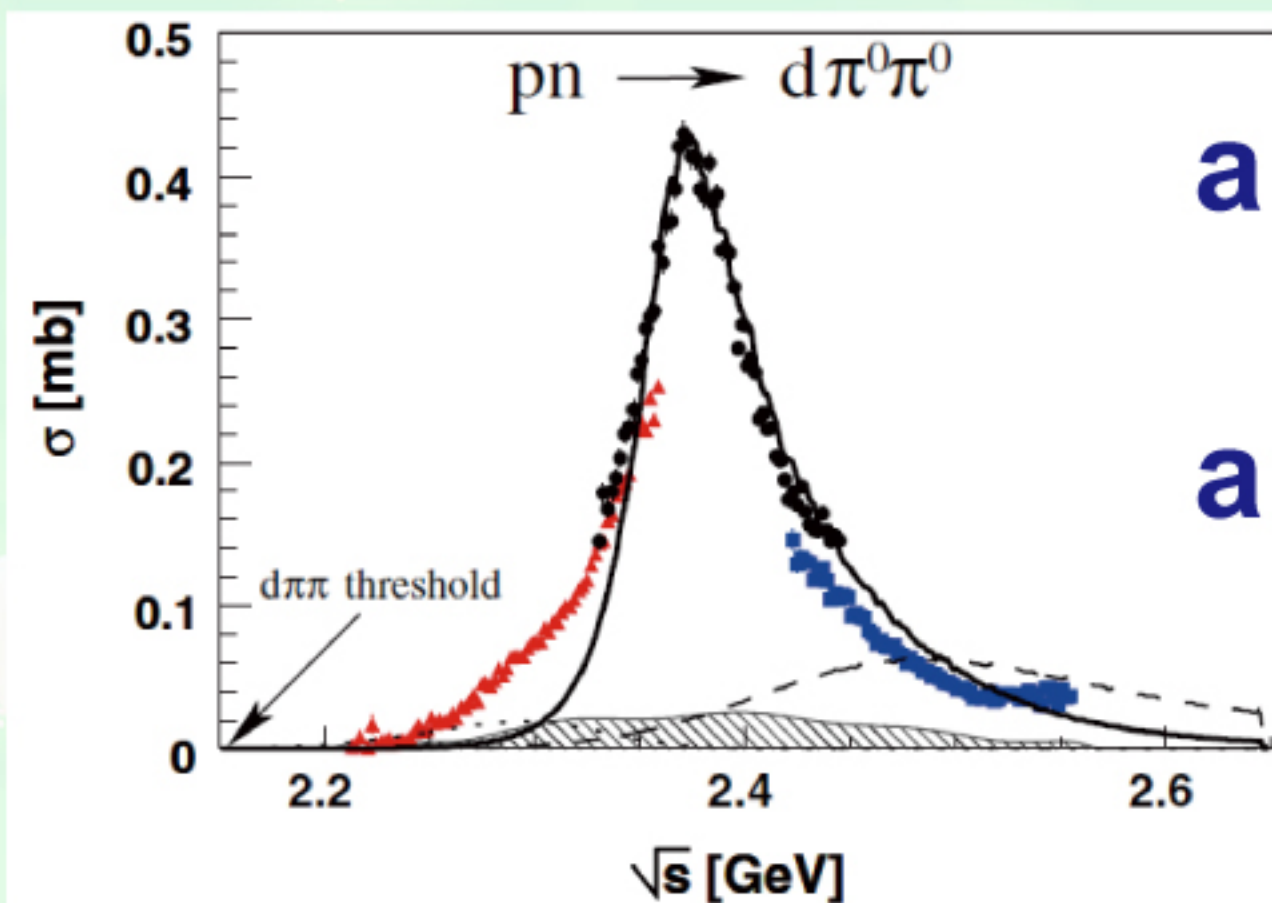
the current problem in hadron physics
insights into the nuclear equation of state
and the interior of a neutron star

$d^*(2380)$

a dibaryon resonance $d^*(2380)$: observed
 $pn \rightarrow \pi^0 \pi^0 d$ reaction

$m=2.37 \text{ GeV}$, $\Gamma=0.07 \text{ GeV}$, $I=0$, $J^\pi=3^+$

M. Bashkanov et al. (CELCIUS/WASA), PRL102, 052301 (2009).
P. Adlarson et al. (WASA-at-COSY), PRL106, 242302 (2011).



a hexaquark state,
and/or
an isoscalar $\Delta\Delta$ quasi-
bound state, \mathcal{D}_{03}

F.J. Dyson and N.-H. Xuong,
PRL13, 815 (1964).



$d^*(2380)$

**F.J. Dyson, N.-H. Xuong,
Phys. Rev. Lett. 13, 815 (1964).**

$d^*(2380)$
|

\mathcal{D}_{IS}	\mathcal{D}_{01}	\mathcal{D}_{10}	\mathcal{D}_{12}	\mathcal{D}_{21}	\mathcal{D}_{03}	\mathcal{D}_{30}
BB	NN	NN	ΔN	ΔN	$\Delta\Delta$	$\Delta\Delta$
M	A	A	$A+6B$	$A+6B$	$A+10B$	$A+10B$
	1878	1878	2160	2160	2348	2348

$$M = A + \{I(I+1) + S(S+1) - 2\}B$$

$$A = 1878 \text{ MeV}$$

$$B = 47 \text{ MeV}$$

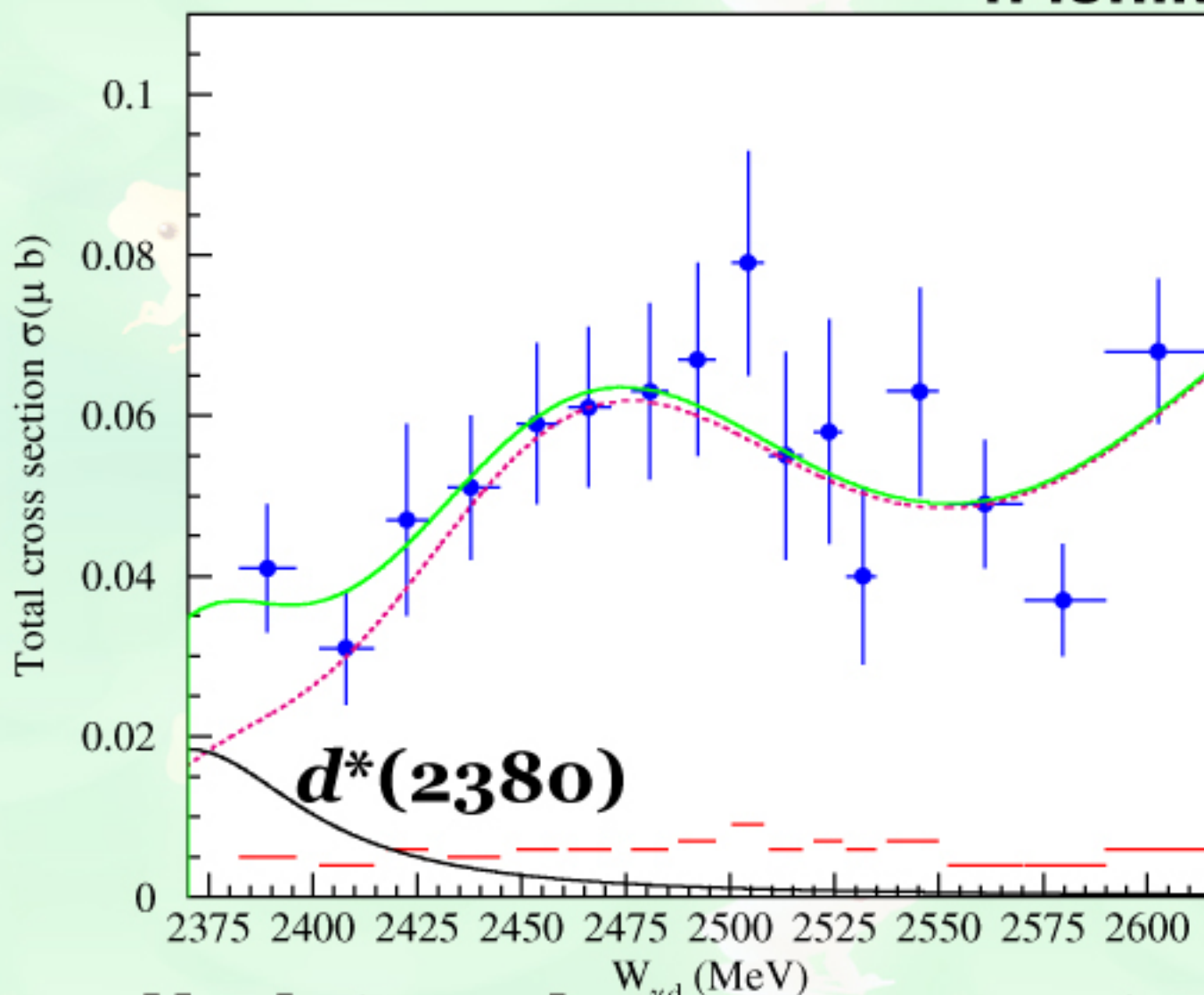
non-attractive
 1S_0 states: pp, pn, nn

deuteron:
attractive 3S_1 state

$d^*(2380)$

total cross section for $\gamma d \rightarrow \pi^0 \pi^0 d$
below the incident energy of 0.88 GeV

T. Ishikawa et al., PLB772, 398 (2017).



Breit-Wigner +
theoretical calculation

A. Fix and H. Arenhobvel,
Euro. Phys. J. A 25, 115 (2005).

Systematic error

a slight enhancement:

18.4±9.2 nb (upper limit: 34 nb 90%CL)



$\mathcal{D}_{12}(2150)$

the excitation spectrum: internal structures of dibaryons

$d^*(2380)$

\mathcal{D}_{IS}	\mathcal{D}_{01}	\mathcal{D}_{10}	\mathcal{D}_{12}	\mathcal{D}_{21}	\mathcal{D}_{03}	\mathcal{D}_{30}
BB	NN	NN	ΔN	ΔN	$\Delta\Delta$	$\Delta\Delta$
M	A	A	$A+6B$	$A+6B$	$A+10B$	$A+10B$
	1878	1878	2160	2160	2348	2348

WASA-at-COSY, PRL121, 052001 (2018)

$$pp \rightarrow \pi^- \pi^+ pp$$

WASA-at-COSY, PLB762, 455 (2016)

$$pp \rightarrow \pi^- \pi^- \pi^+ \pi^+ pp$$

$\mathcal{D}_{12}(2150)$

\mathcal{D}_{12} : partial-wave analysis

$\pi d \rightarrow pp$: R. Arndt et al., PRC48, 1926 (1993).

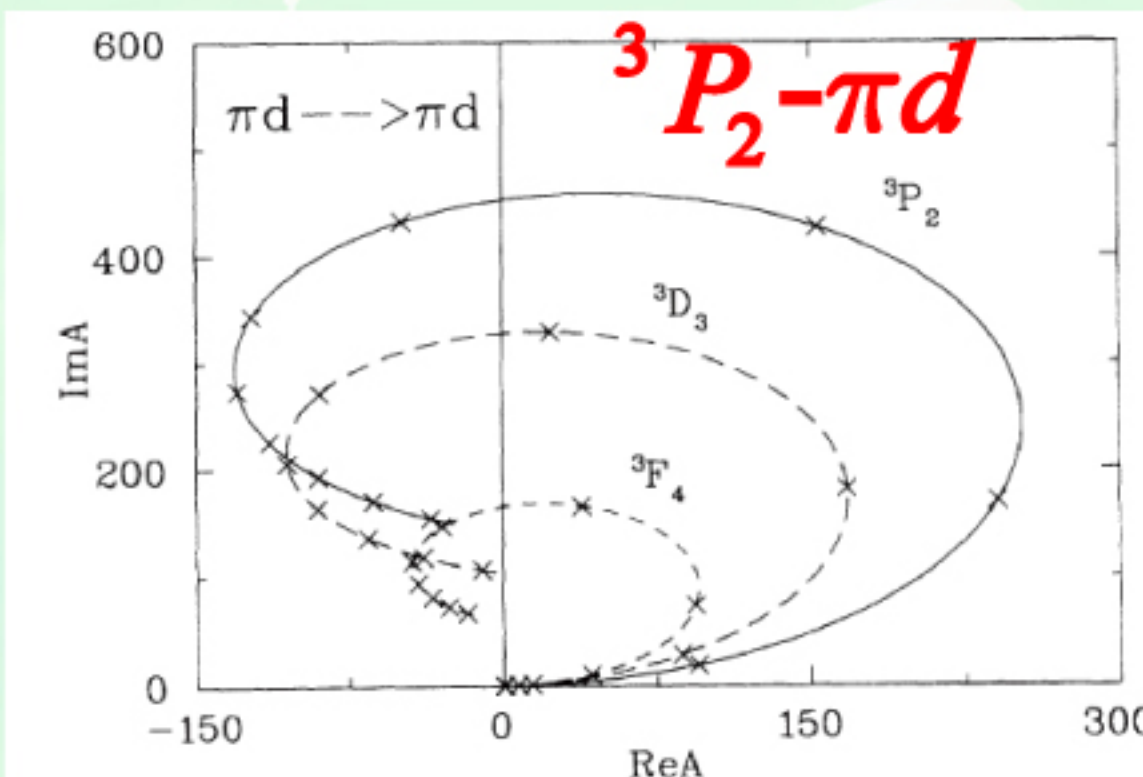


FIG. 7. Argand plot of the dominant πd partial-wave amplitudes 3P_2 , 3D_3 , and 3F_4 which correspond to the 1D_2 , 3F_3 , and 1G_4 pp states, respectively. (Compare Fig. 7 of Ref. [3]). The X points denote 50 MeV steps. All amplitudes have been multiplied by a factor of 10^3 .

$\pi d \rightarrow \pi d$: R. Arndt et al., PRC50, 1796 (1994).

The SAID group provides a pole for \mathcal{D}_{12} from a combined analysis including pp elastic scattering.

C.H. Oh et al., PRC56, 635 (1997).

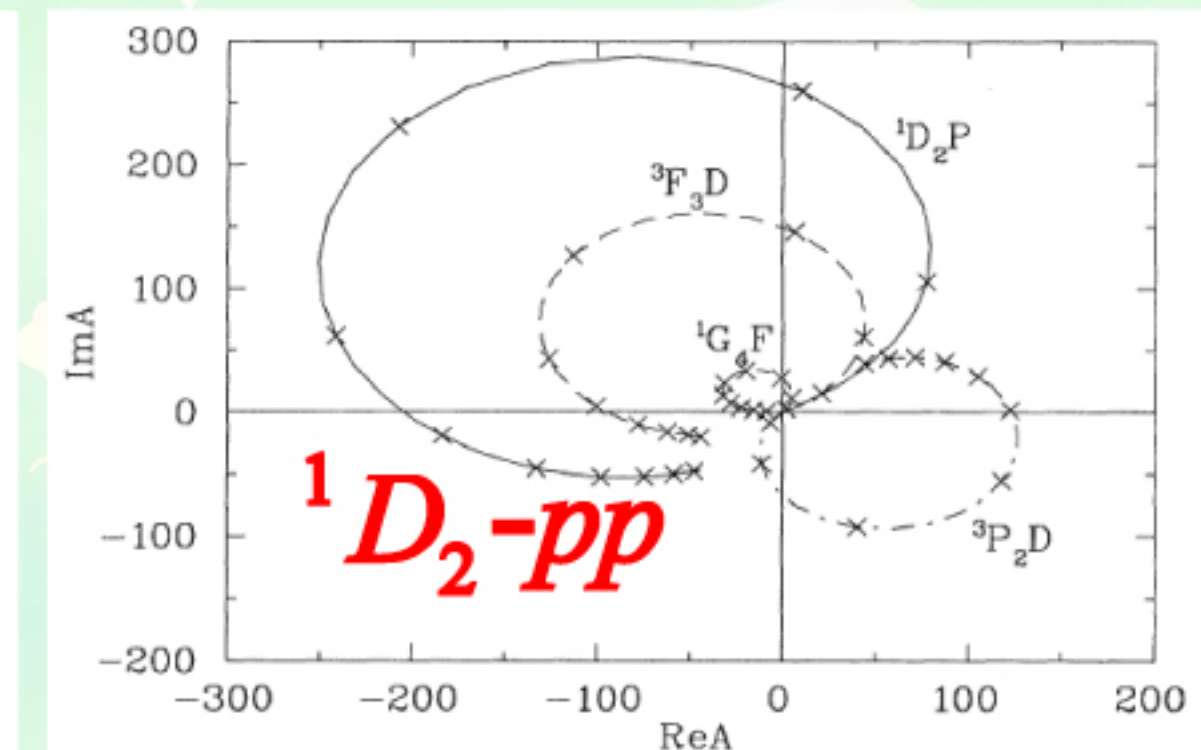
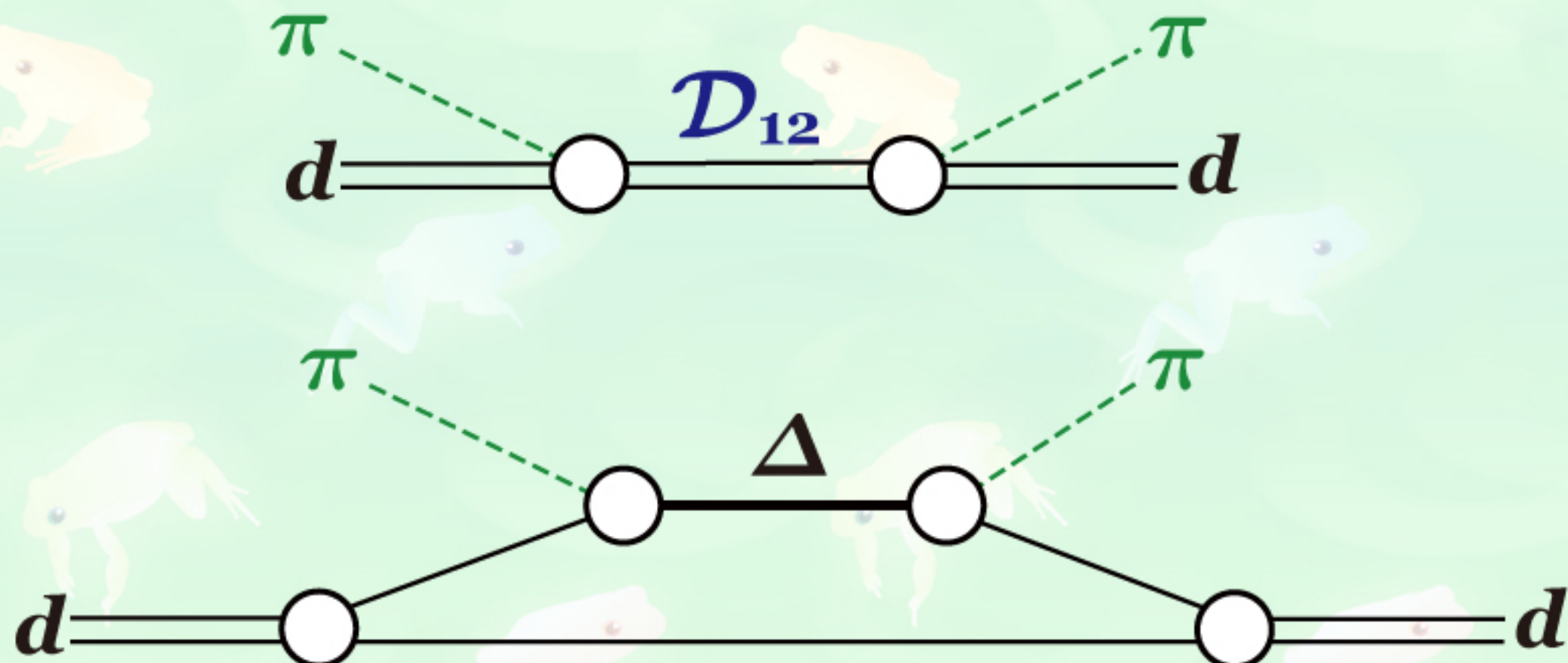


FIG. 7. Argand plot of dominant partial-wave amplitudes. The X points denote 50 MeV steps. All amplitudes have been multiplied by a factor of 10^3 .



$\mathcal{D}_{12}(2150)$

\mathcal{D}_{12} : partial-wave analysis
dibaryonic interpretation is still
questionable

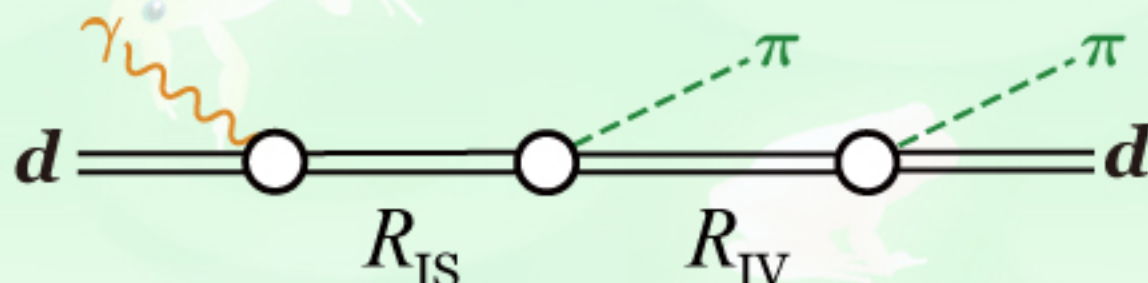


**quasi-free Δ excitation cannot
be kinematically separated**



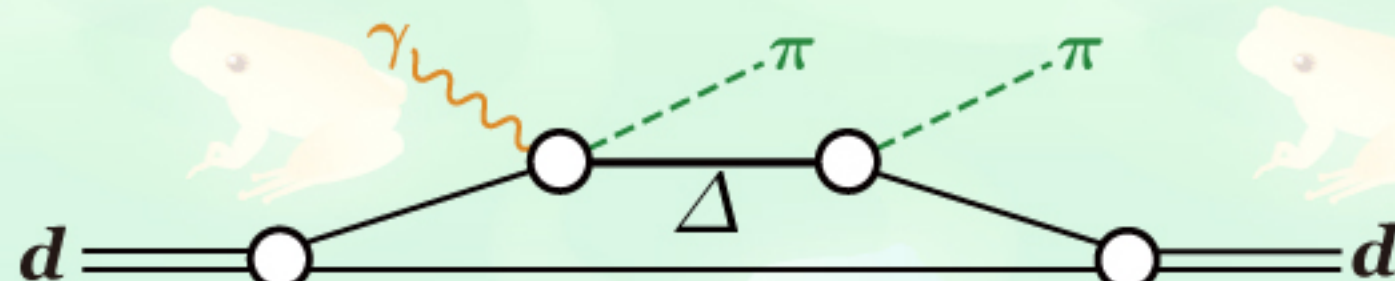
$\gamma d \rightarrow \pi^0 \pi^0 d$ to study \mathcal{D}_{12} (2150)

(1) dibaryon production



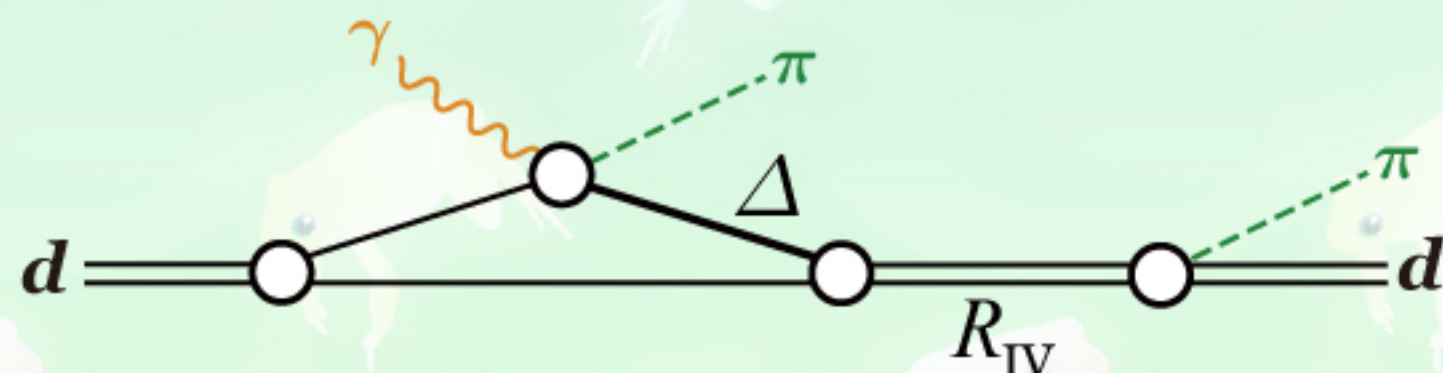
angular distribution of deuteron emission
almost flat

(2) QF $\pi\pi$ production



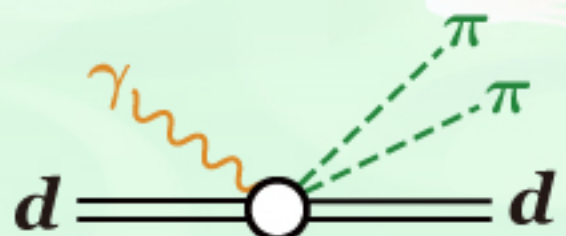
backward peaking

(3) QF $\pi\pi$ production



sideway peaking

(4) QF $\pi\pi$ production



almost flat

kinematically separable!



Accelerator

Electron Beam

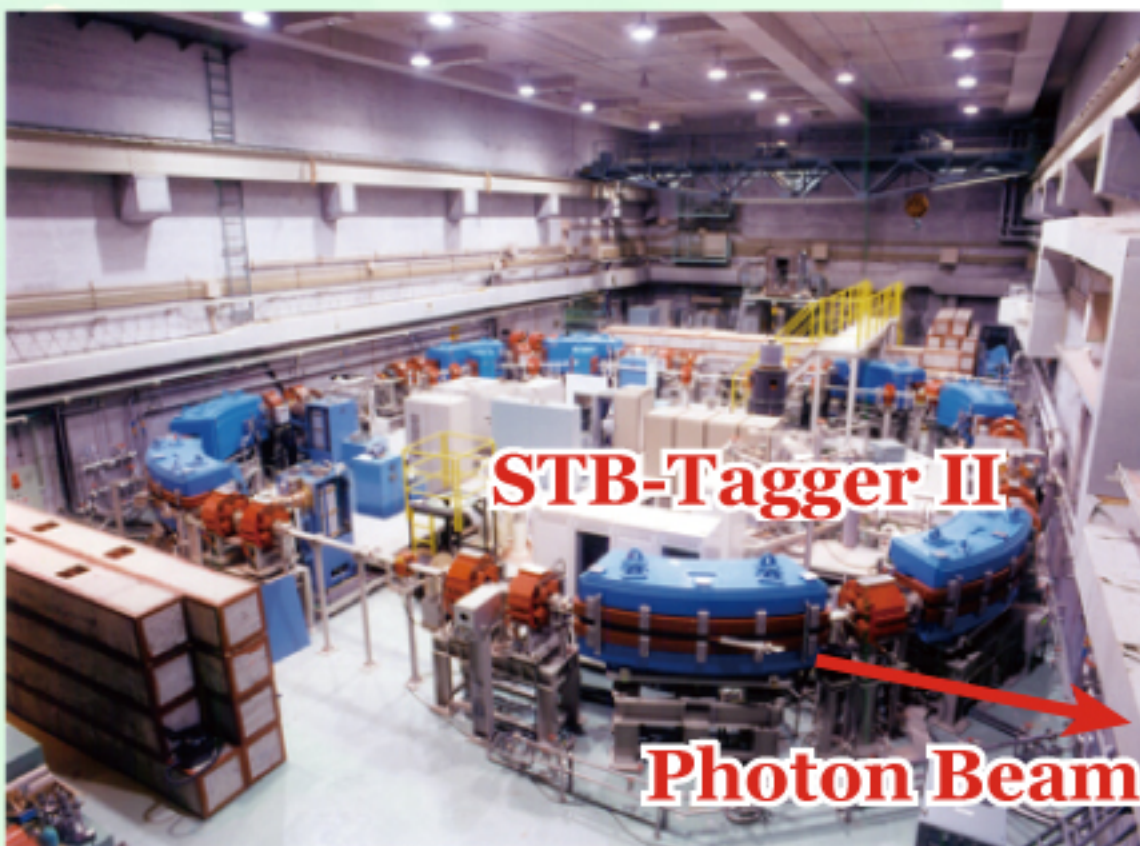
LINAC 150 MeV

Booster Ring 1200 MeV (max)

Photon Beam

Bremsstrahlung

Tagged



1.3 GeV Booster STorage Ring



T. Ishikawa et al., NIMA 622, 1 (2010); T. Ishikawa et al., NIMA 811, 124 (2016);
Y. Matsumura et al., NIMA 902, 103 (2018); Y. Obara et al., NIMA 922, 108 (2019).



EM calorimeter

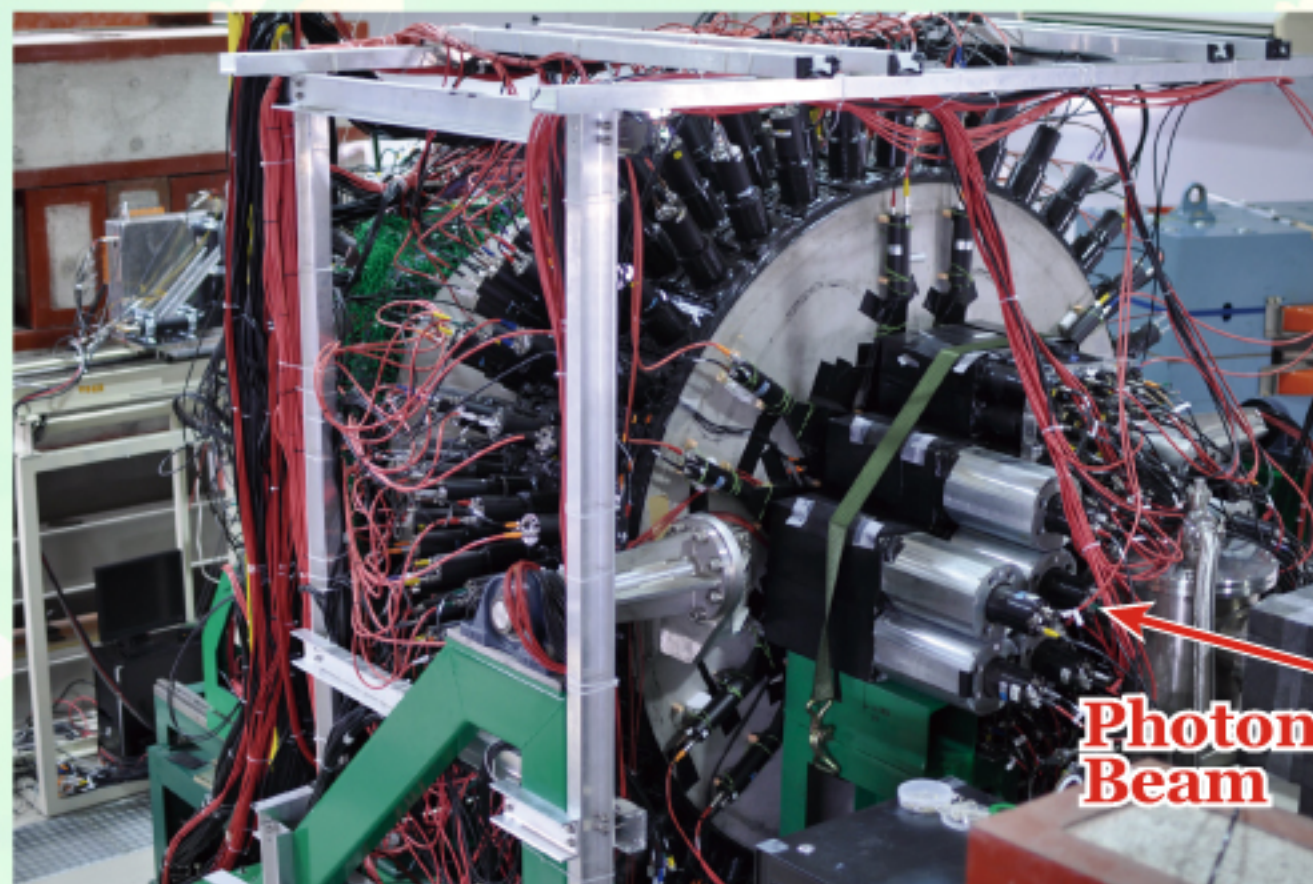
Backward Gamma

SCISSORS III SPIDER



192 CsI crystals
3% @ 1 GeV

252 Lead/SciFi modules
7% @ 1 GeV

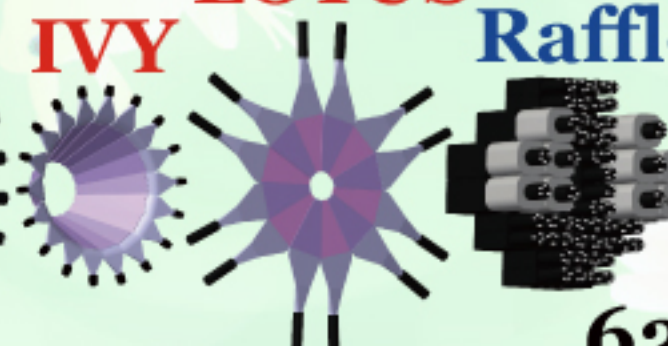


Target: 45 mm thick LH₂ & LD₂

T. Ishikawa et al., NIMA 832, 108 (2016).

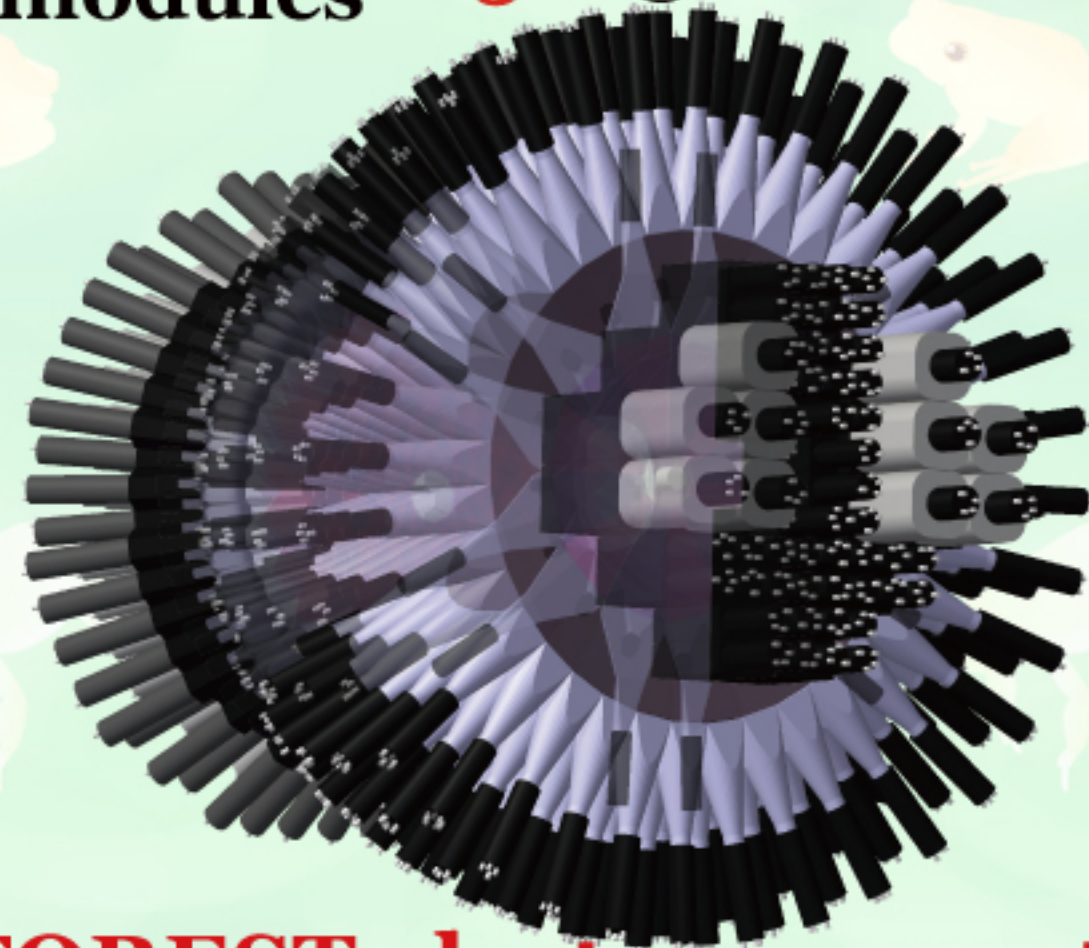
T. Ishikawa, 11 Jun. 2019 (NSTAR2019)

LOTUS Rafflesia II



Photon Beam

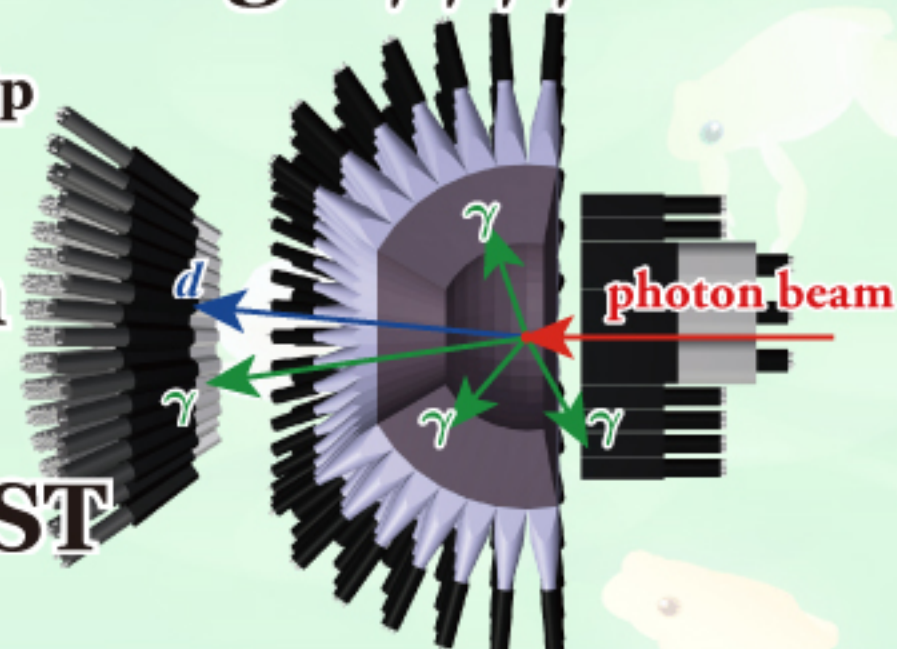
62 Lead Glasses
5% @ 1 GeV



FOREST electro-magnetic
calorimeter

Event Selection

1. 4 neutral particles and 1 charged particle
2. each neutral pion: $\gamma\gamma$ decay
time difference is less than $3\sigma_t$
between every 2 neutral clusters out of 4
3. d is detected with SPIDER
(response of SCISSORS III is not required)
time delay is larger than 1 ns wrt average $\gamma\gamma\gamma\gamma$ time
energy deposit is higher than $2E_{\text{mip}}$
4. sideband background subtraction
to remove accidental coincidence
between STB-Tagger II and FOREST



Event Selection

Further event selection:

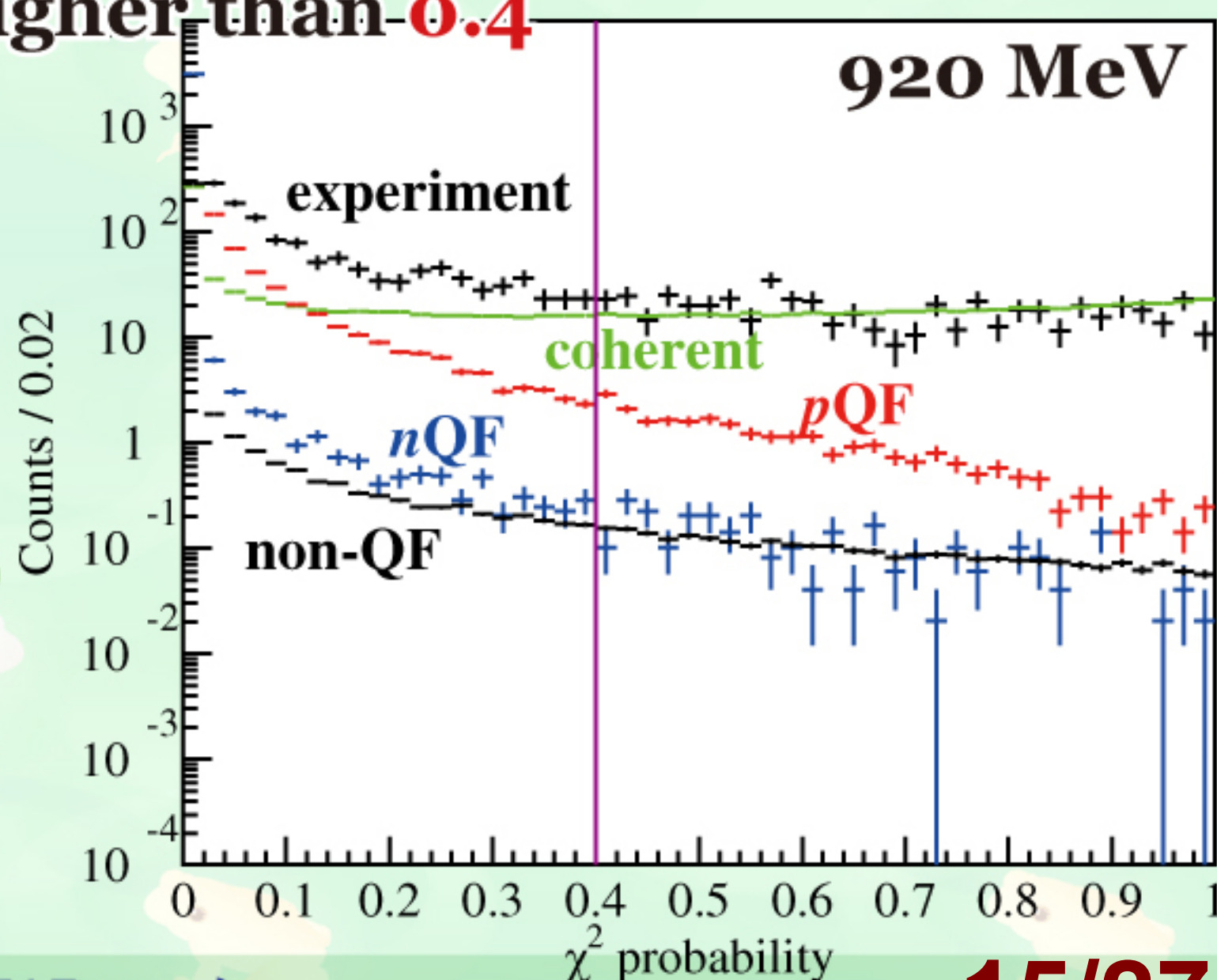
- a kinematic fit with 6 constraints is applied
- energy and momentum conservation (4)
- each $\gamma\gamma$ invariant mass is m_{π^0} (2)
- χ^2 probability is higher than **0.4**

$\gamma d \rightarrow \pi^0 \pi^0 d$ (coherent)

$\gamma p' \rightarrow \pi^0 \pi^0 p$ (pQF)

$\gamma n' \rightarrow \pi^0 \pi^0 n$ (nQF)

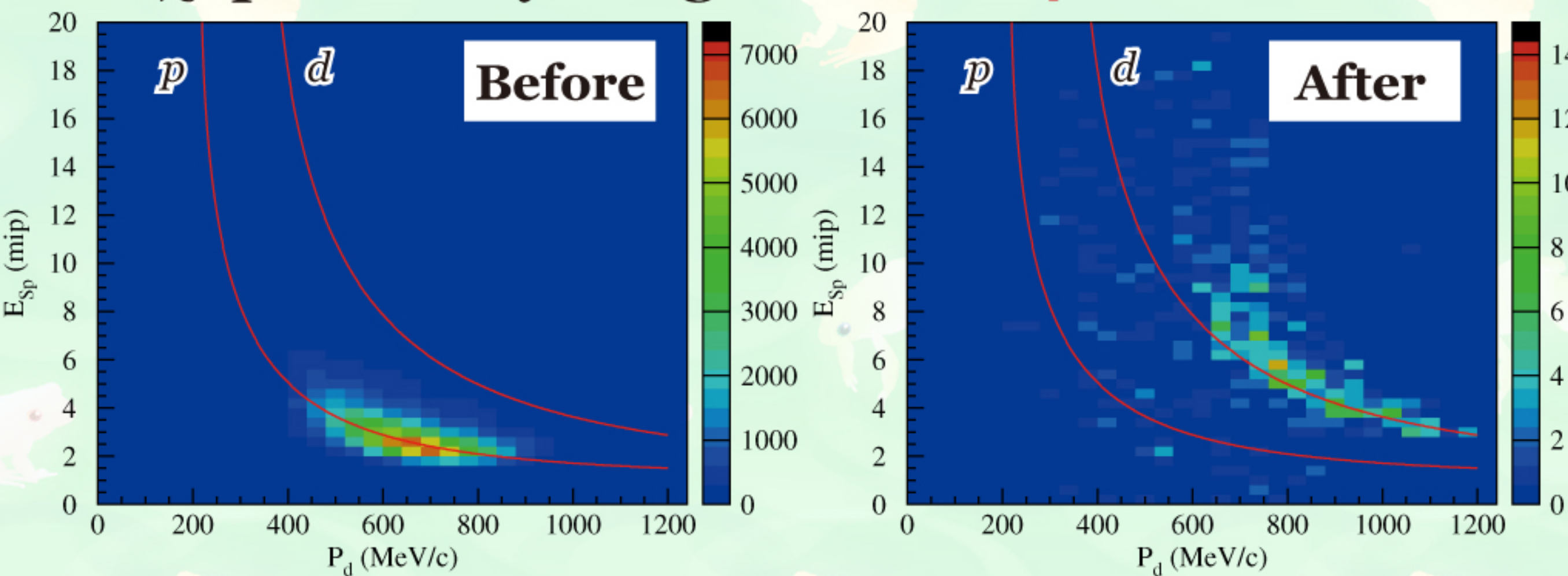
$\gamma d \rightarrow \pi^0 \pi^0 pn$ (non QF)



Event Selection

Further event selection:

a kinematic fit with 6 constraints is applied
energy and momentum conservation (4)
each $\gamma\gamma$ invariant mass is m_{π^0} (2)
 χ^2 probability is higher than **0.4**

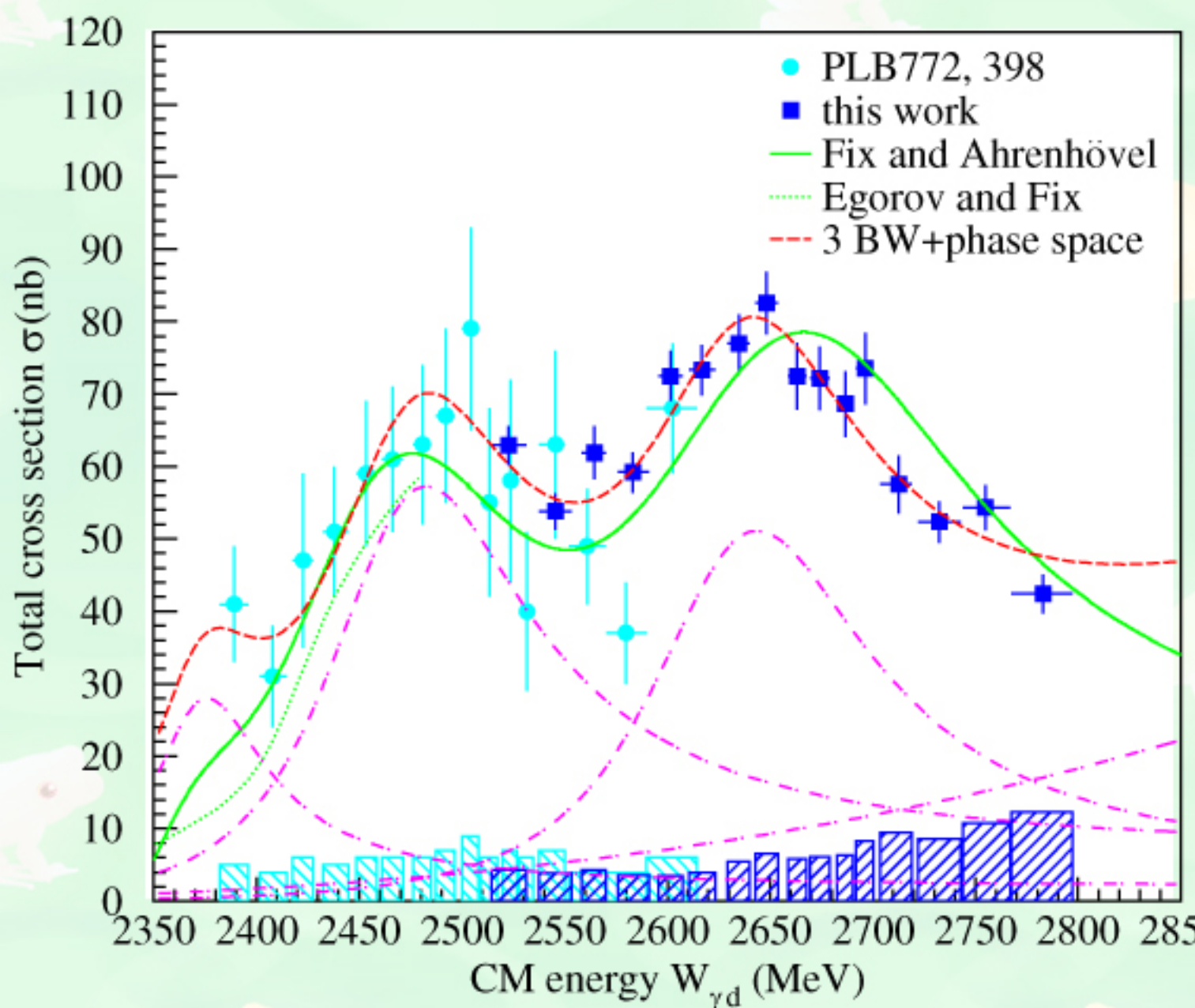


missing momentum is given for the deuteron in these plots

Total cross section

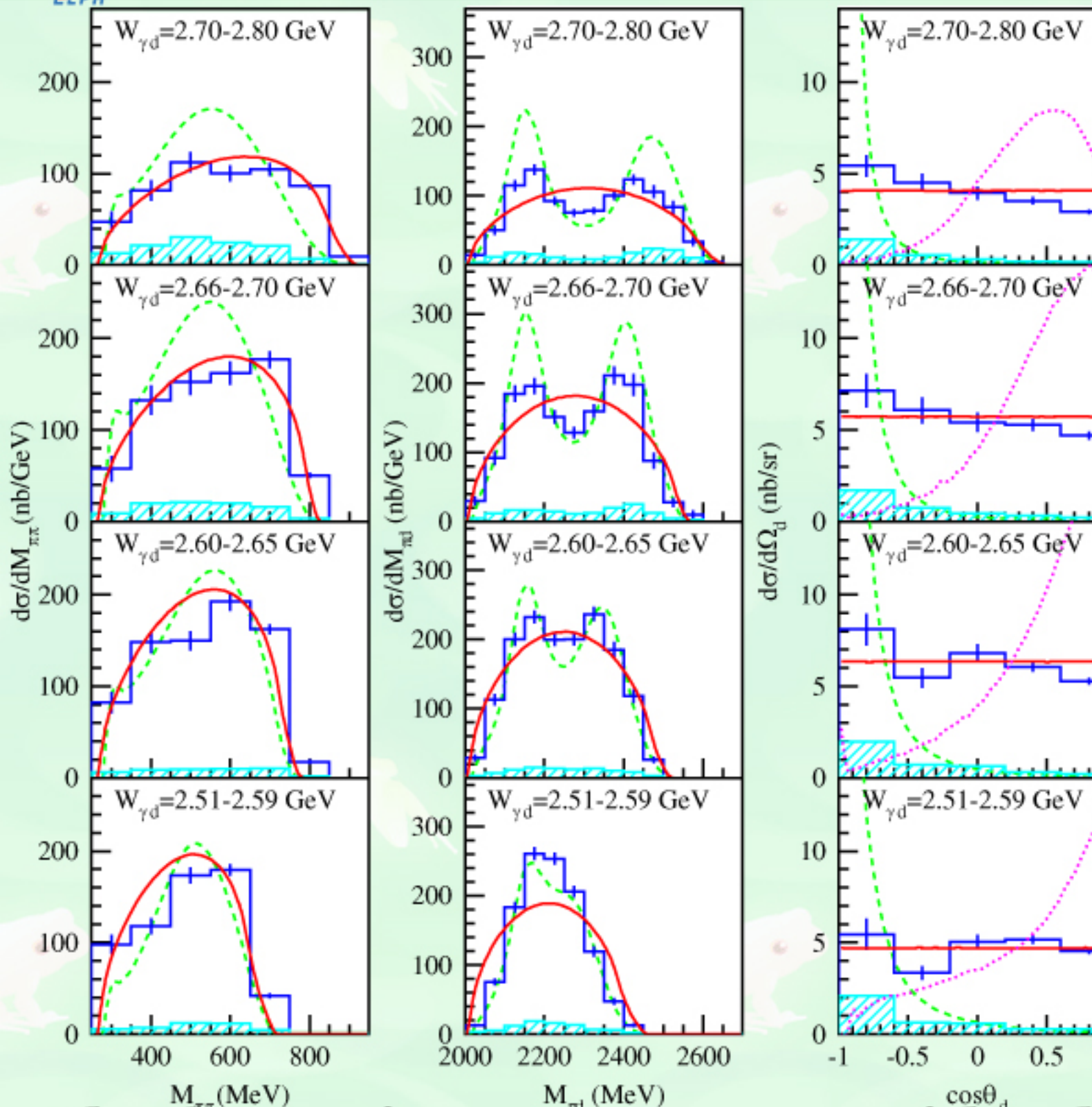
total cross section for $\gamma d \rightarrow \pi^0 \pi^0 d$

at the incident energy 0.55~1.15 GeV



resonance-like behavior
peaked at around 2.47 and
2.63 GeV
two-peak structure is similar
to the excitation function of
QF $\pi\pi$ production
corresponding to the second-
and third-resonance regions
of the nucleon
naiive interepretation:
QF excitation of the nucleon

Differential cross section



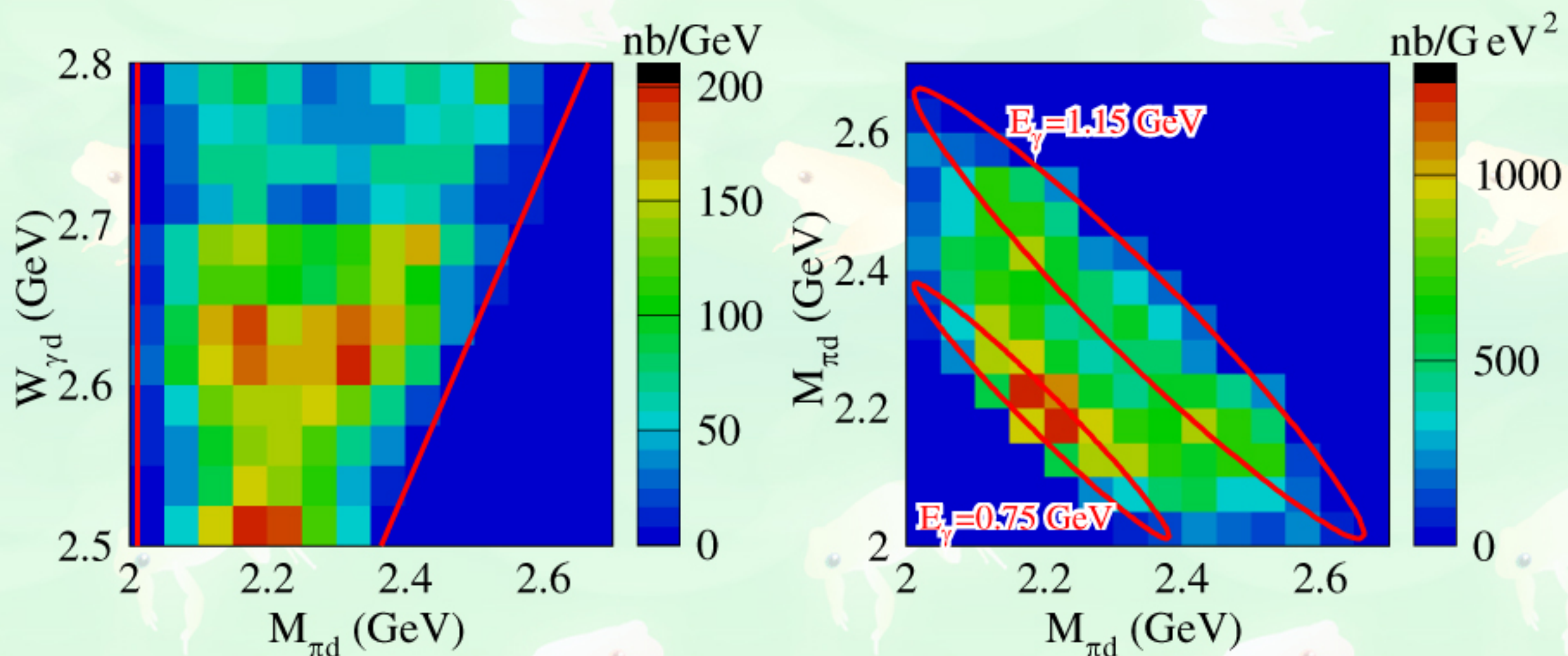
$\pi^0 d$ invariant mass
a peak at ~ 2.15 GeV
and its reflection

deuteron emission
rather flat
slight backward peaking
at high energies

The data points are compare with calculations
by Fix and Arenhövel (FA calculation).
T. Ishikawa, 11 Jun. 2019 (NSTAR2019)

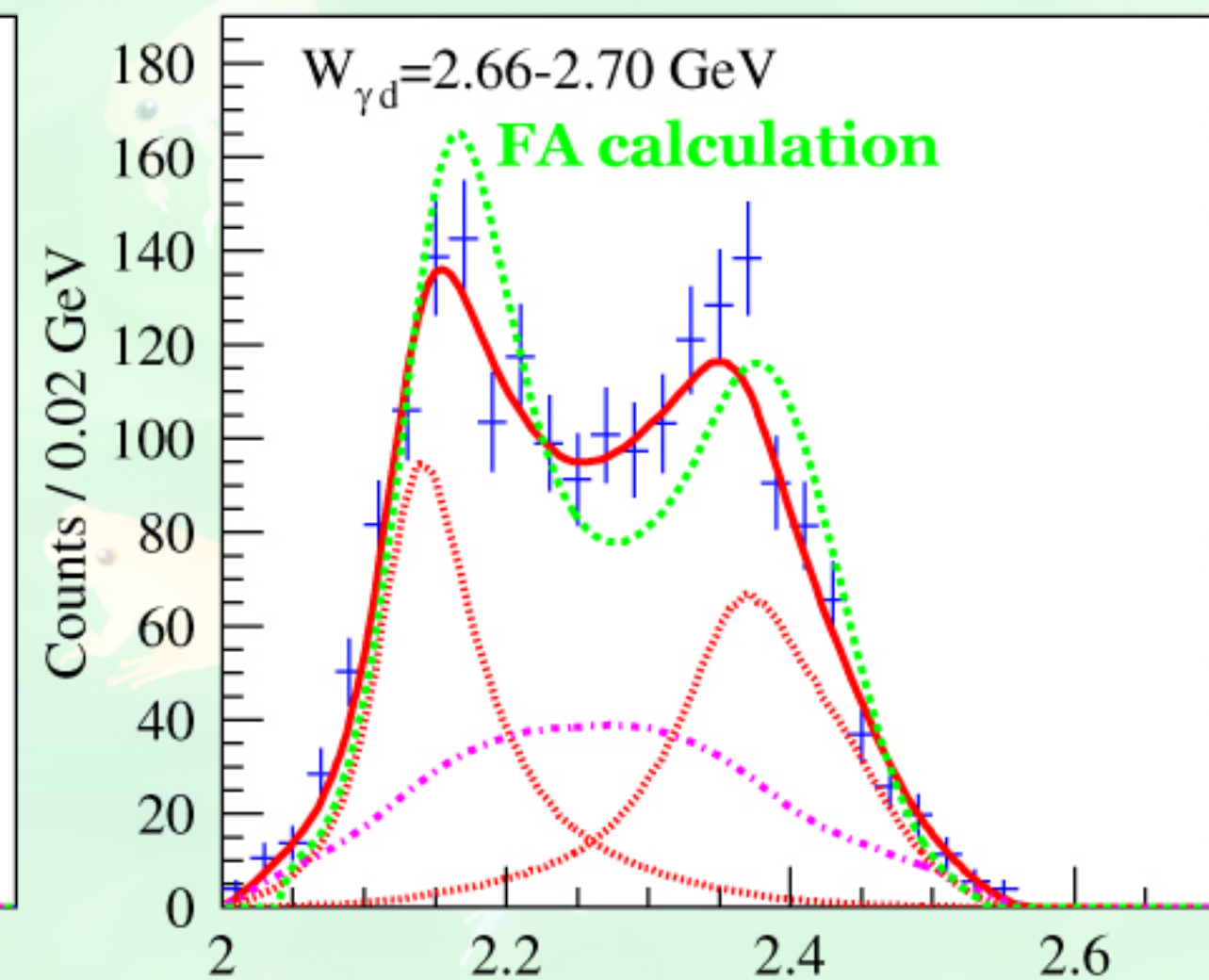
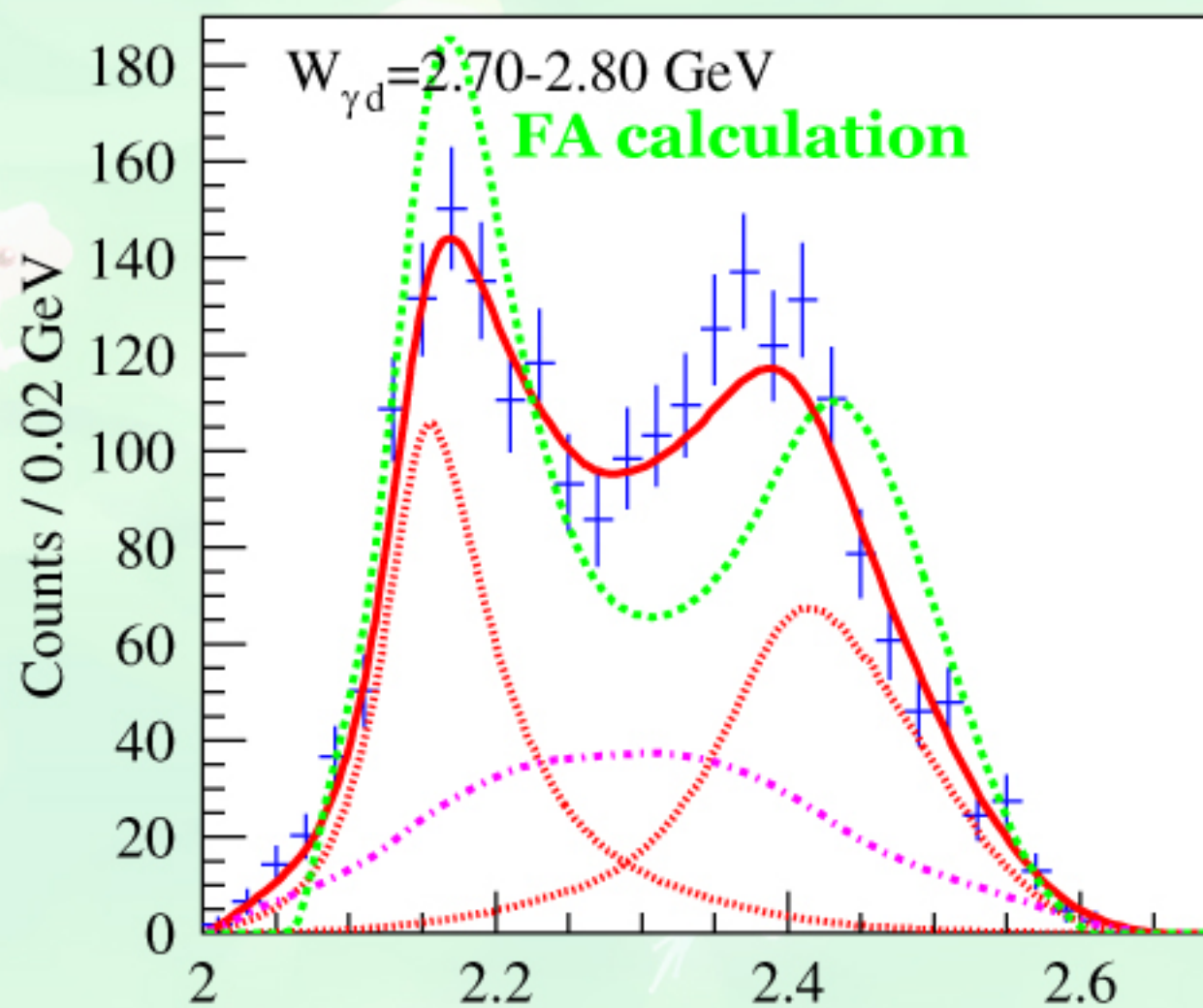
πd invariant mass

loci corresponding to \mathcal{D}_{12} can be observed
in correlation plots.



available region is very limited
at a fixed incident energy

πd invariant mass



$$N(m_1) = \int_{m_2} \left(\alpha \left| L_{M,\Gamma}(m_1) + L_{M,\Gamma}(m_2) \right|^2 + C \right) V_{\text{PS}}(m_1, m_2) dm_2$$

convoluted with 11-MeV- σ Gaussian

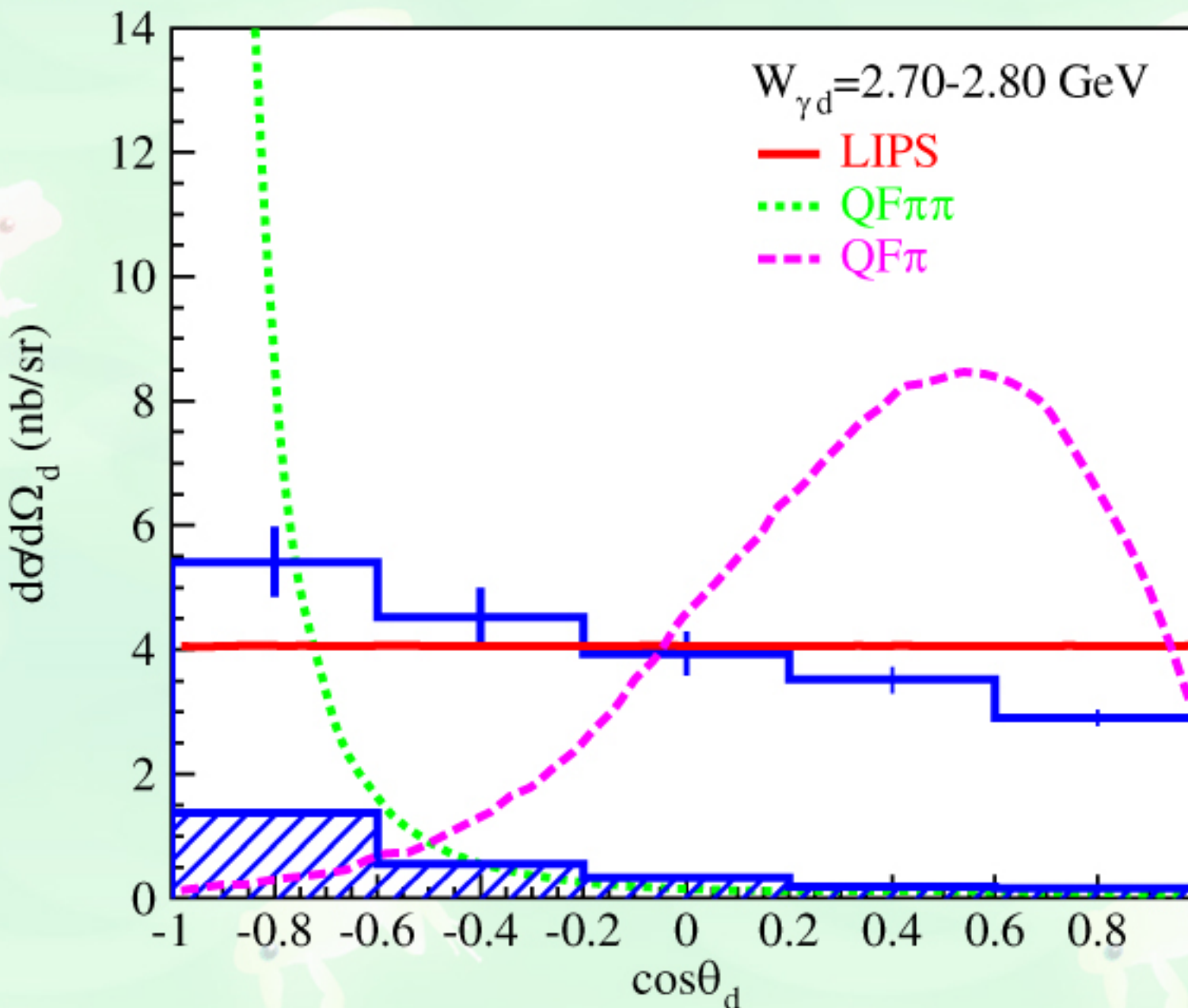
Breit-Wigner amplitude:

$$L_{M,\Gamma}(m) = \left(m^2 - M^2 + iM\Gamma \right)^{-1}$$

mass $2140 \pm 11 \text{ MeV}$ & width $91 \pm 11 \text{ MeV}$

\mathcal{D}_{12} or $\Delta + N$

deuteron angular distribution

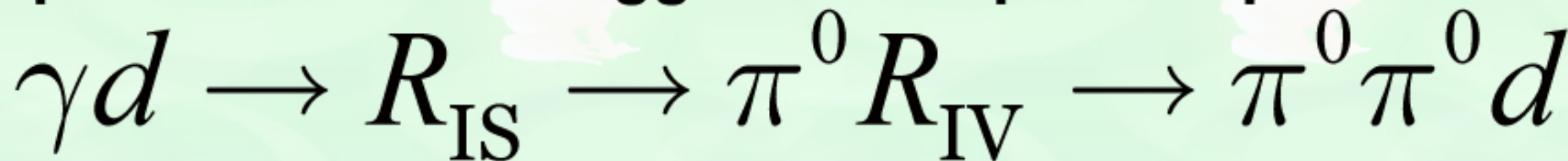


QF $\pi\pi$ production
(FA calculation)

QF π production

pure phase space
(direct $\pi\pi$ production)

- experimental data suggests a sequential process:

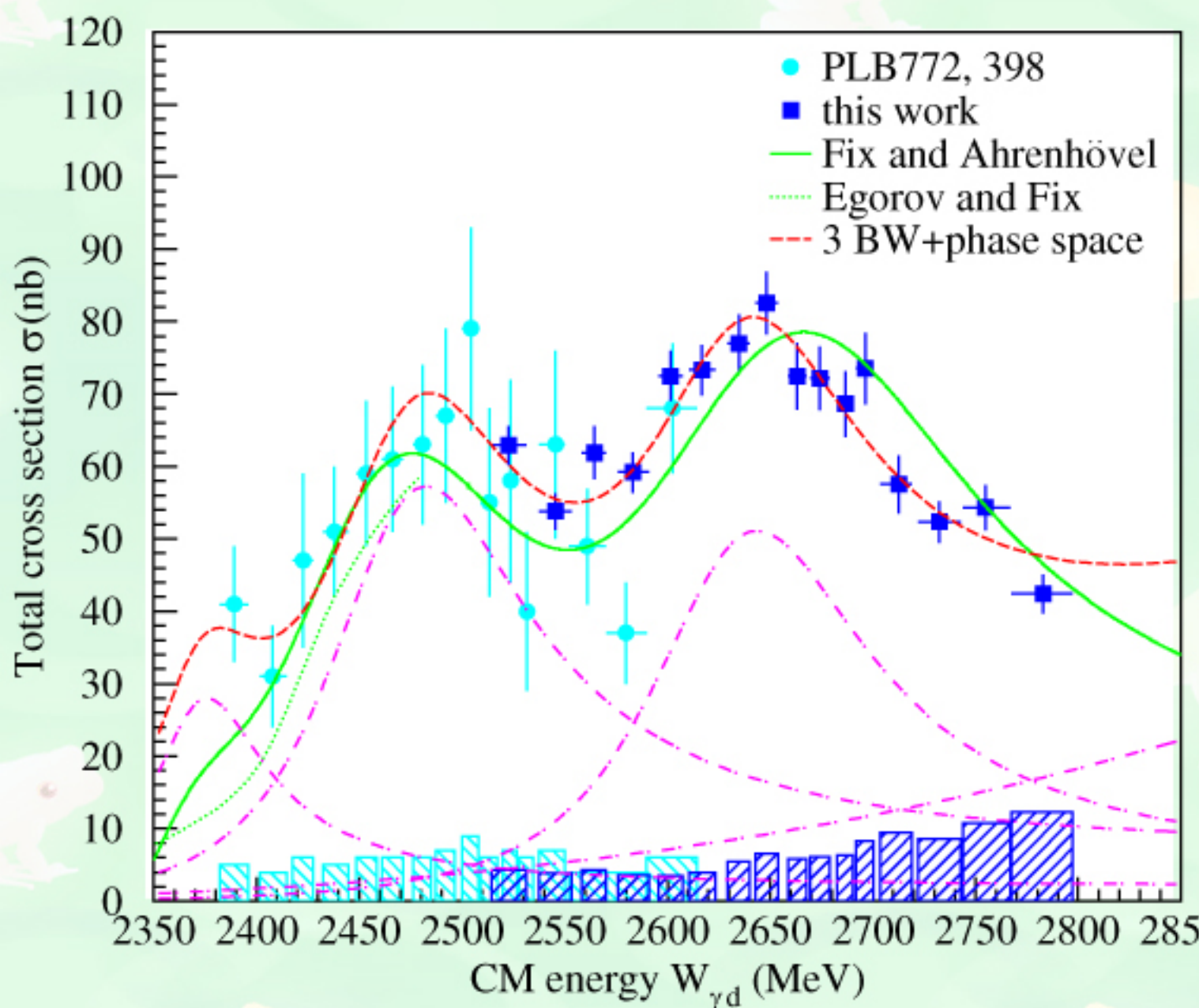


(rather flat angular distribution & 2.15-GeV peak in $M_{\pi d}$)

Total cross section

total cross section for $\gamma d \rightarrow \pi^0 \pi^0 d$

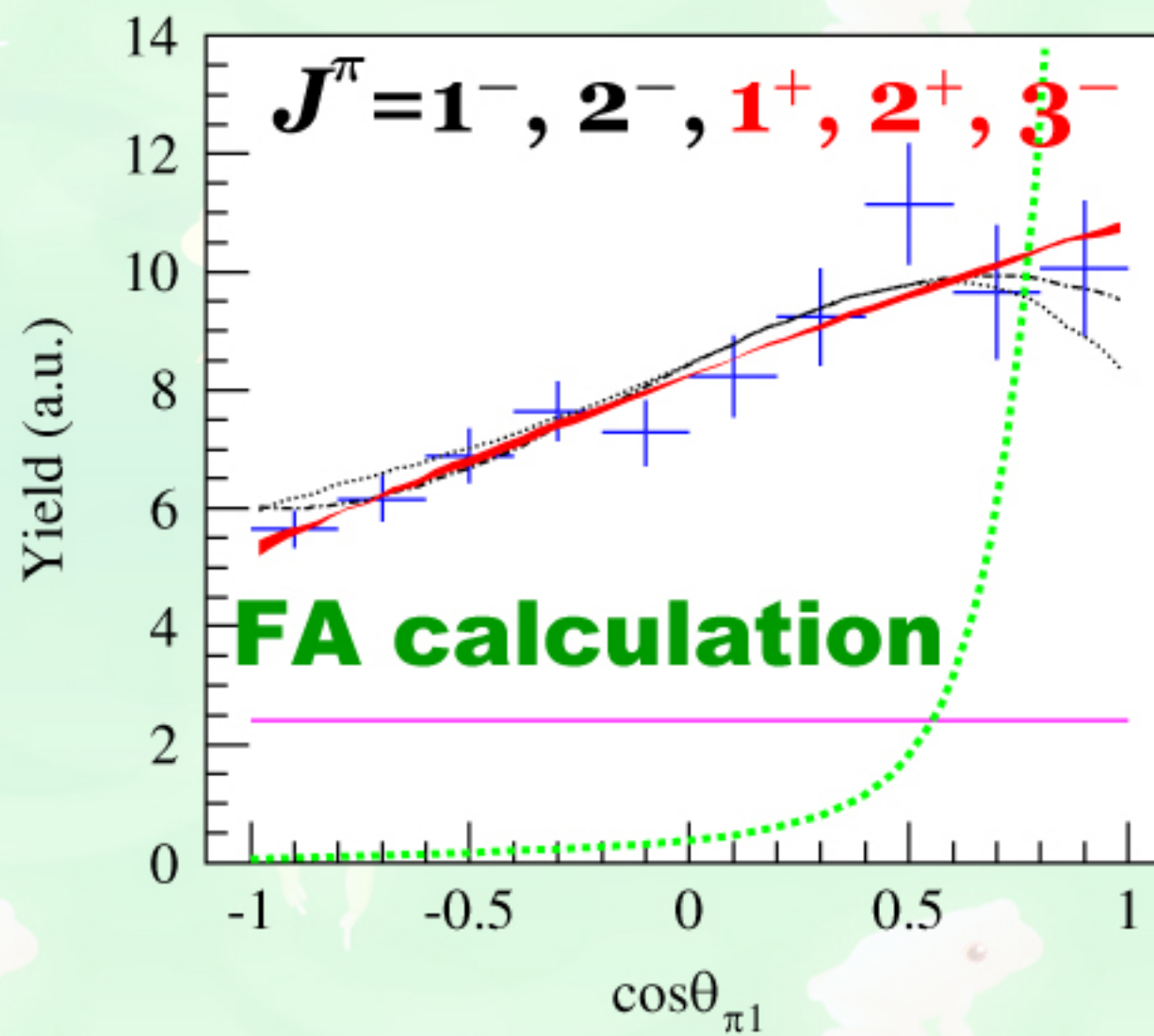
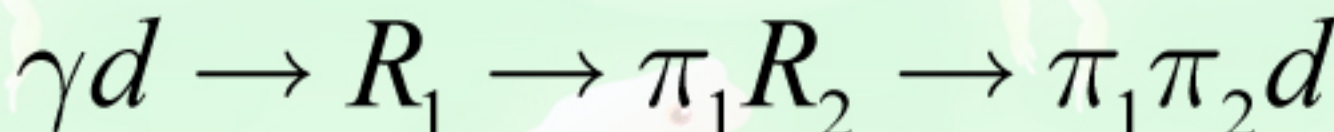
at the incident energy 0.55~1.15 GeV



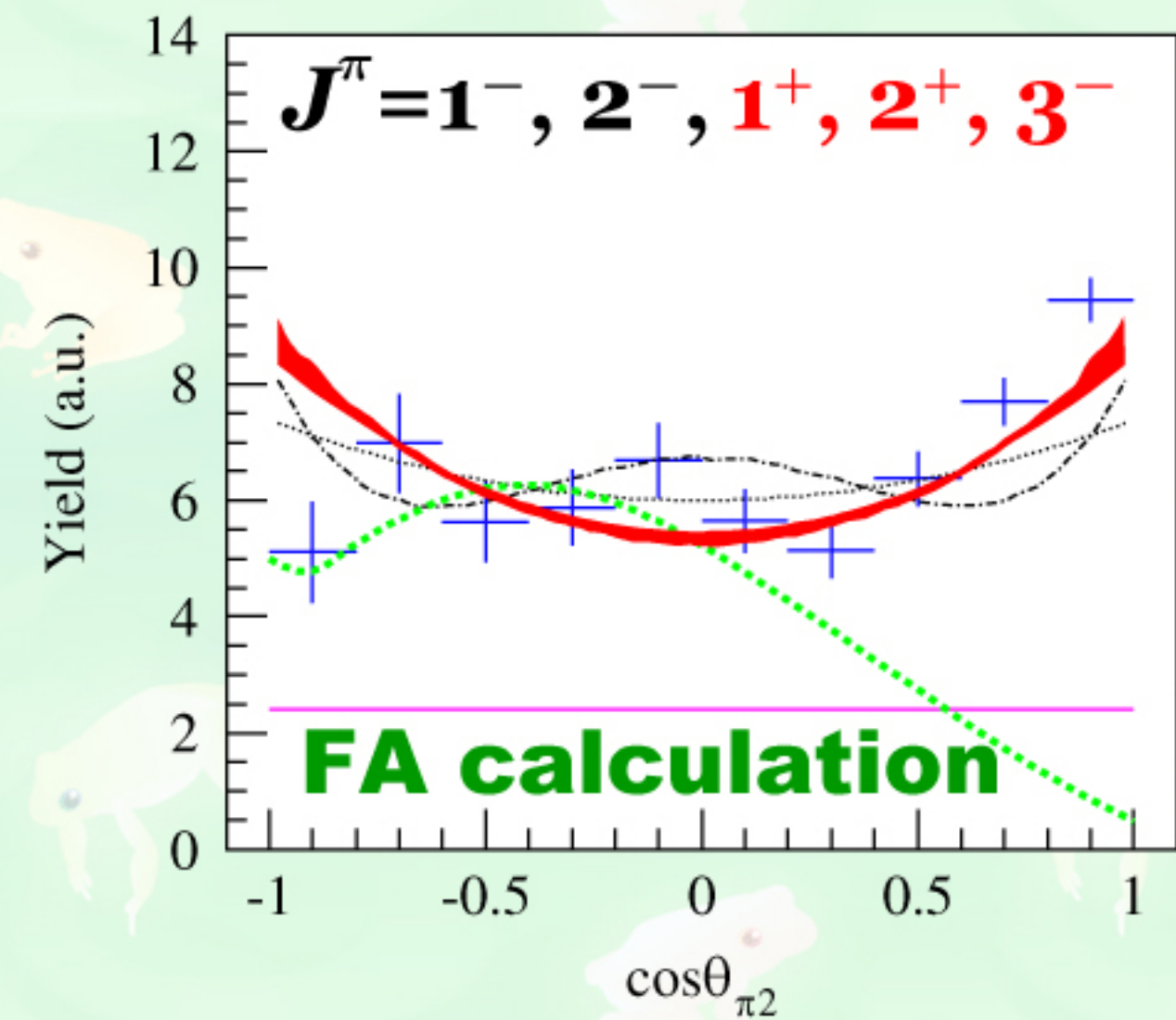
resonance-like behavior
peaked at around 2.47 and
2.63 GeV

3 dibaryons:
2.38, 2.47, and 2.63 GeV
with widths of
0.07, 0.12, 0.13 GeV

Spin and parity sequential process:



π_1 emission angle
in the γd CM frame
z axis: γ



π_2 emission angle
in the $\pi_2 d$ rest frame
z axis: opposite to π_1



Excitation spectrum

$NP_{13}(1720)$ 2.62~2.66

$NF_{15}(1680)$ 2.62~2.66

$ND_{15}(1675)$ 2.62~2.66

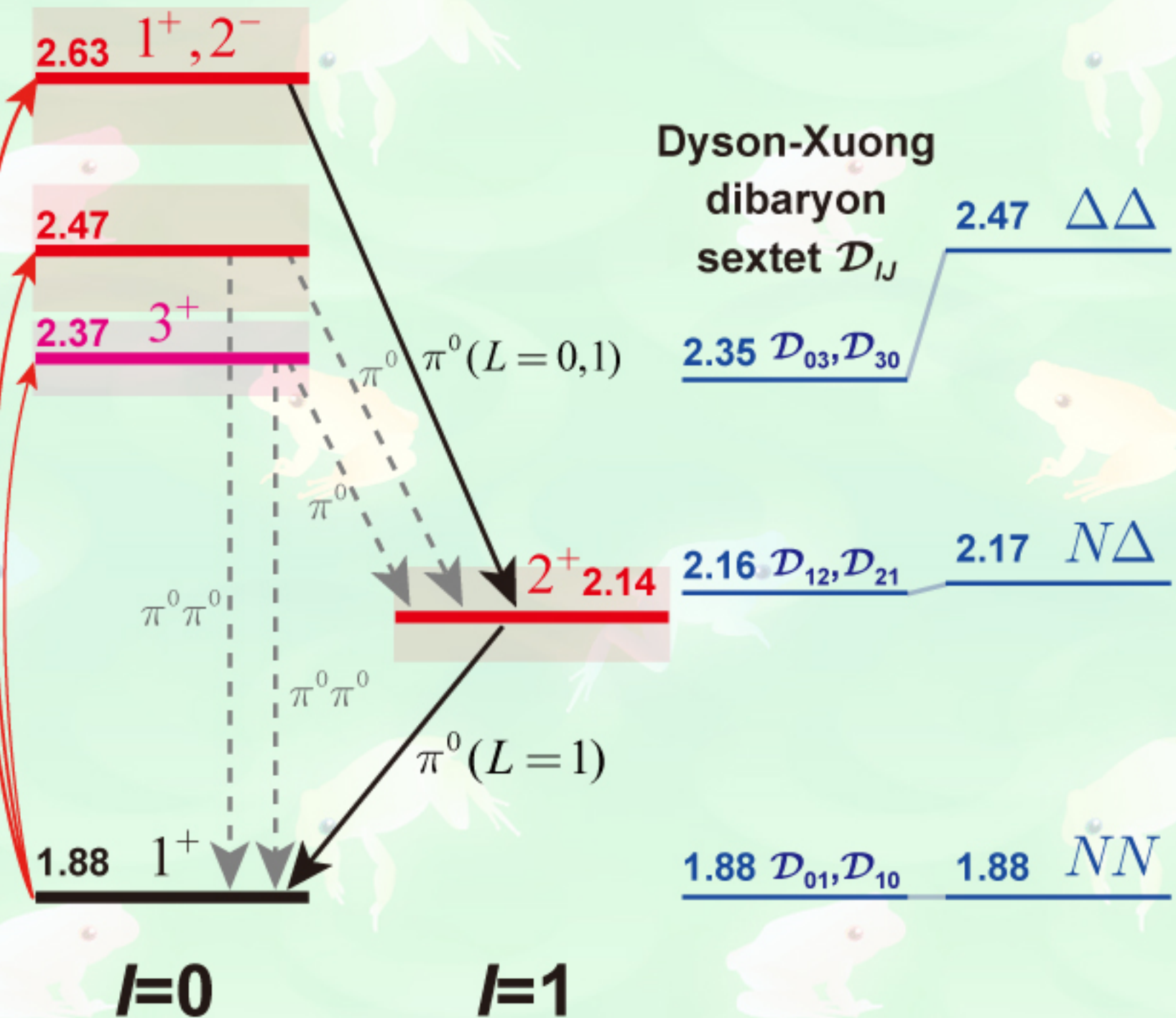
$NS_{11}(1535)$ 2.46~2.47

$ND_{13}(1520)$ 2.46~2.47

$NP_{11}(1440)$ 2.38

doorway states?

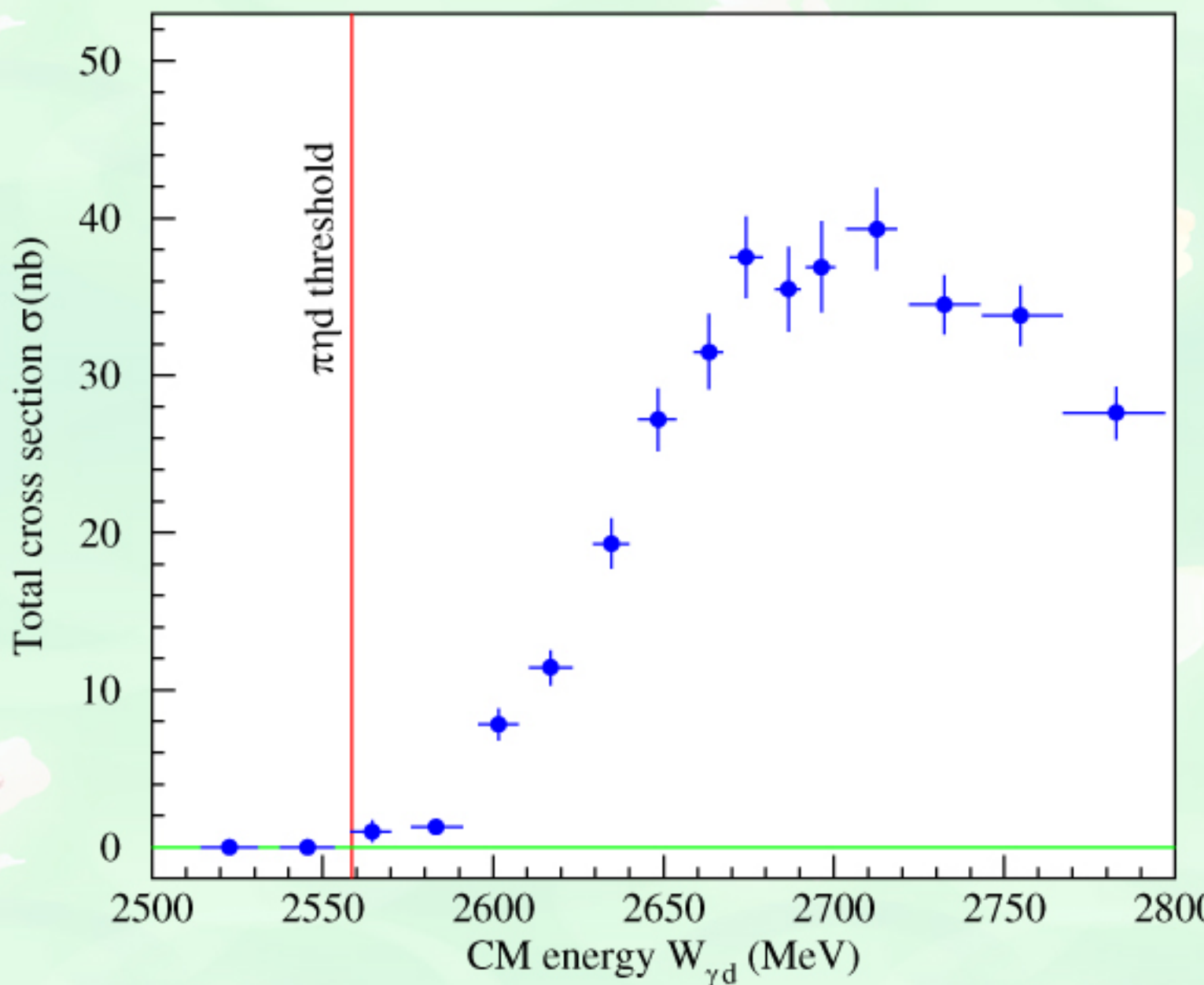
photo-excitation



Two isoscalar dibaryons and an isovector dibaryons are observed in the $\pi\pi d$ and πd systems, respectively.

$\gamma d \rightarrow \pi^0 \eta d$ TCS

total cross section for $\gamma d \rightarrow \pi^0 \eta d$
at the incident energy 0.74~1.15 GeV

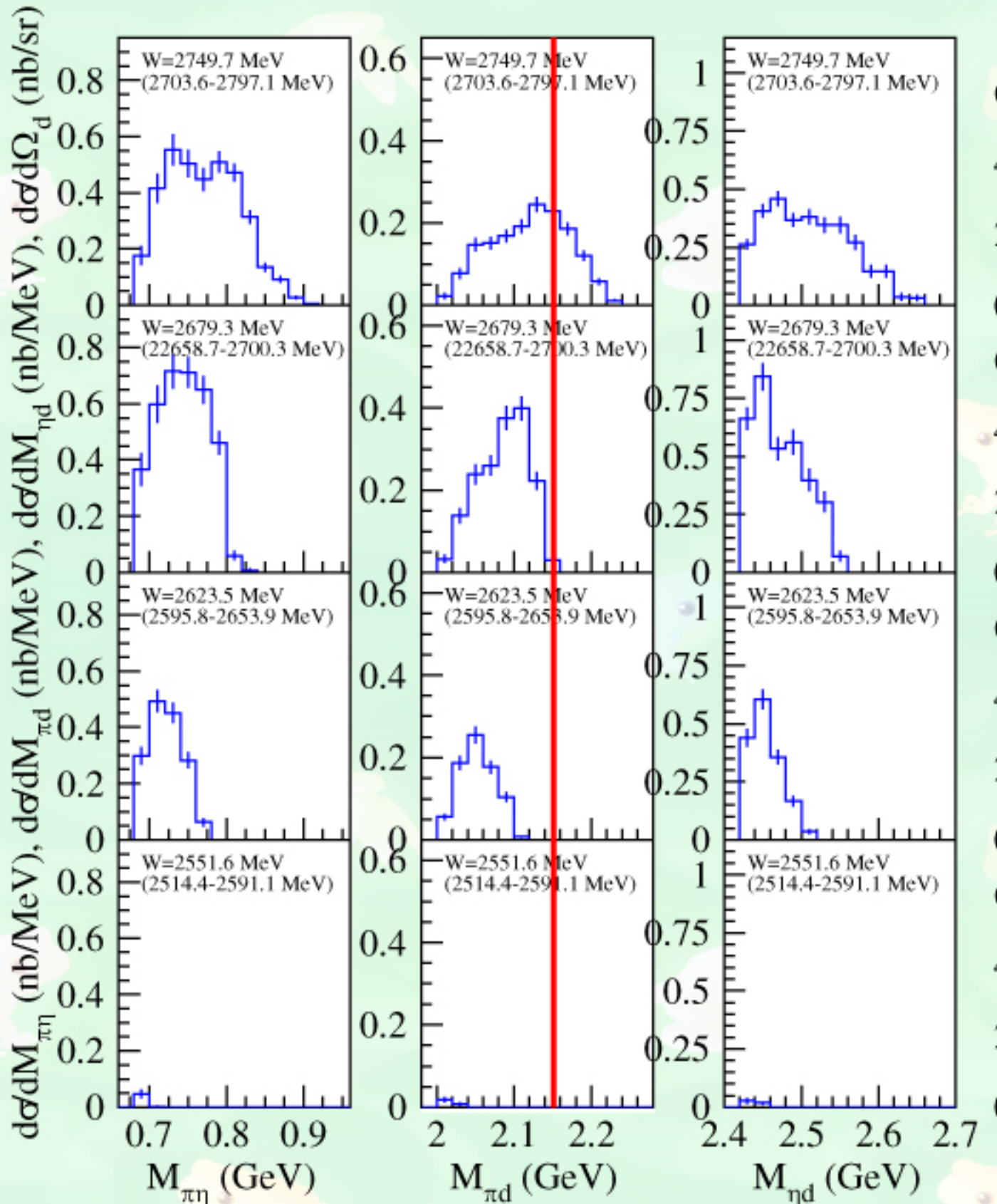


angular distribution of
deuteron emission:
rather flat

isovector dibaryon?



$\gamma d \rightarrow \pi^0 \eta d$ DCS



**angular distribution of
deuteron emission:
rather flat**

**πd invariant mass
shows a peak at
2.15 GeV.**



Summary

Total cross section of the $\gamma d \rightarrow \pi^0 \pi^0 d$ reaction has been measured at $W_{\gamma d} = 2.38 \sim 2.80$ GeV for the first time.
A slight enhancement corresponding to $d^*(2380)$ $\sim D_{03}$ candidate~ is observed.

T. Ishikawa et al., PLB772, 398 (2017).

Additional two dibaryon resonances are observed at 2.47 and 2.63 GeV with widths of 0.12 and 0.13 GeV
(A rather flat angular distribution of deuteron emission shows production of dibaryon resonances).

A peak at $M \sim 2.15$ GeV $\sim D_{12}$ candidate~ is observed in the $\pi^0 d$ invariant mass distribution for the $\gamma d \rightarrow \pi^0 \pi^0 d$ reaction at $W_{\gamma d} = 2.50 \sim 2.80$ GeV.

$M = 2.14 \pm 0.01$ GeV, $\Gamma = 0.09 \pm 0.01$ GeV

$J^\pi = 1^+, 2^+$ or 3^-

T. Ishikawa et al., PLB789, 413 (2019).